Steel and Composite Structures, *Vol. 34, No. 3 (2020) 377-391*
DOI: https://doi.org/10.12989/scs.2020.34.3.377

Numerical study on the axial compressive behavior of built-up CFT columns considering different welding lines

Mahdi Shariati[1,2a], Morteza Naghipour[3b], Ghazaleh Yousofizinsaz[3c], Ali Toghroli*[4] and Nima Pahlavannejad Tabarestani[3d]

[1]*Division of Computational Mathematics and Engineering, Institute for Computational Science, Ton Duc Thang University, Ho Chi Minh City, Vietnam*
[2]*Faculty of Civil Engineering, Ton Duc Thang University, Ho Chi Minh City, Vietnam*
[3]*Department of Civil, Babol Noshirvani University of Technology, Babol, Iran*
[4]*Institute of Research and Development, Duy Tan University, Da Nang 550000, Viet Nam*

(*Received April 24, 2019, Revised September 15, 2019, Accepted September 24, 2019*)

Abstract. A concrete filled steel tube (CFT) column with stiffeners has preferable behavior subjected to axial loading condition due to delay local buckling of the steel wall than traditional CFT columns without stiffeners. Welding lines in welded built-up steel box columns is expected to behave as longitudinal stiffeners. This study has presented a numerical investigation into the behavior of built-up concrete filled steel tube columns under axial pressure. At first stage, a finite element model (FE) has been built to simulate the behavior of built-up CFT columns. Comparing the results of FE and test has shown that numerical model passes the desired conditions and could accurately predict the axial performance of CFT column. Also, by the raise of steel tube thickness, the load bearing capacity of columns has been increased due to higher confinement effect. Also, the raise of concrete strength with greater cross section is led to a higher load bearing capacity compared to the steel tube thickness increment. In CFT columns with greater cross section, concrete strength has a higher influence on load bearing capacity which is noticeable in columns with more welding lines.

Keywords: built-up CFT; welding lines; stiffeners; FEM; strength

1. Introduction

A close shape of steel built-up sections has appropriate behavior under seismic loading and is a desirable choice for structural members in buildings (Khorami *et al.* 2017a, Khorami *et al.* 2017b, Zhang *et al.* 2018, Chen *et al.* 2019, Mortazavi *et al.* 2020). The intelligently combination of these sections with concrete has provided a cost and time reduction in building construction (Han *et al.* 2014, Judd *et al.* 2018, Kildashti *et al.* 2019). Nowadays, steel-concrete composite columns are widely applied in high-rise buildings and bridges with long spans because of their great strength, stiffness and higher energy absorption capacity than traditional steel and concrete columns (Jalali *et al.* 2017).

*Corresponding author, Ph.D.
E-mail: alitoghroli@duytan.edu.vn
[a]Ph.D.
E-mail: shariati@tdtu.edu.vn
[b]Professor
E-mail: m-naghi@nit.ac.ir
[c]MSC.
E-mail: ghyousefi@yahoo.com
[d]Ph.D.
E-mail: nimapnt@gmail.com

CFT columns use the beneficial properties of both concrete and steel (Arabnejad Khanouki *et al.* 2010, Arabnejad Khanouki *et al.* 2011, Arabnejad Khanouki *et al.* 2016). Concrete core delays the occurrence of local buckling and prevents inward local buckling in steel tube wall (Fig. 1), while the steel tube would prevent the lateral expansion of filled concrete like stirrups and increase the compressive strength of concrete core through confinement effect (Shariati *et al.* 2013a, Gupta *et al.* 2014, Luo *et al.* 2019, Sajedi *et al.* 2019, Xie *et al.* 2019). These types of composite sections are used in fast construction without removing any formwork and usually connected to the reinforced concrete or steel beams to construct an efficient lateral resisting frame system (Fig. 2).

CFT members have been used in china such as the main columns of metro stations in Beijing since 1966 and also in the power plants building since 1970 or recently in SEG tower in Shenzhen province, Rongfeng international trade fair in Hangzhou, Canton tower in Guangzhou, Higgo building in Kobe city of japan, Gateway building in US, Fifty five floor Millennium building in Australia and bank of china in Hong Kong (Han *et al.* 2014). Different papers have been studied the dynamic response of the mide-rise building, and composite structures under seismic events (Jalali *et al.* 2012, Ahmadi *et al.* 2016, Kildashti *et al.* 2019, Mortazavi *et al.* 2020), also different types of loading scenarios as full-cyclic, half cyclic, reversed cyclic, and shack table have employed to evaluate structural behavior of the specimens in full-scale or

ISSN: 1229-9367 (Print), 1598-6233 (Online)

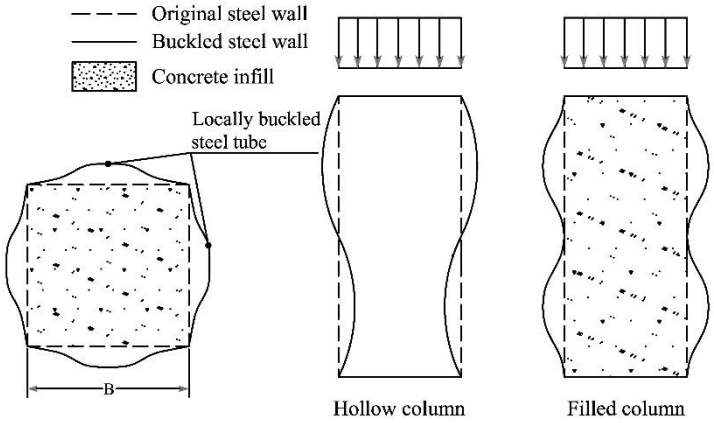

Fig. 1 Local buckling in hollow and CFT sections (Ahmadi *et al.* 2019)

Fig. 2 Lateral resisting frame system with CFT column (Han *et al.* 2014)

half-scale tests (Shariati *et al.* 2012a, Shariati *et al.* 2012b, Shariati *et al.* 2012c, Shariati 2013, Shariati *et al.* 2013b, Mohammadhassani *et al.* 2014, Shariati *et al.* 2014a, Shariati *et al.* 2014b, Khorramian *et al.* 2015, Shariati *et al.* 2015, Shariati *et al.* 2016, Tahmasbi *et al.* 2016, Ismail *et al.* 2018, Nasrollahi *et al.* 2018, Paknahad *et al.* 2018, Shariati *et al.* 2018, Wei *et al.* 2018, Davoodnabi *et al.* 2019). An empirical finite element (FE) study on load carrying capacity of thin and composite steel–concrete stubs subjected to direct compression has been performed including one I-shaped steel section or two cold formed U-shaped steel plates welded to form a steel box (Zeghiche 2013).

There are different available techniques for data validations and predictions such as employing artificial neural networks (Safa *et al.* 2016, Sadeghipour Chahnasir *et al.* 2018, Chuanhua Xu 2019, Katebi *et al.* 2019, Shariati *et al.* 2019a, Shariati *et al.* 2019b, Trung *et al.* 2019b), Finite element method (Daie *et al.* 2011, Shariati *et al.* 2011, Khorramian *et al.* 2017, Mahdi Shariati 2019, Taheri *et al.* 2019, Usefi *et al.* 2019), Finite strip method (Sinaei *et al.* 2011, Shao *et al.* 2015, Sharafi *et al.* 2018a, Sharafi *et al.* 2018b, Shariati *et al.* 2020b, Shariati *et al.* 2020a, Sharafi *et al.* 2018c, Shi *et al.* 2019) and other specific smart ways of analysis in civil engineering area (Shah *et al.* 2015, Shariat *et al.* 2018, Zandi *et al.* 2018, Ziaei-Nia *et al.* 2018). Finite element method which is generally carried out by FE programs as ABAQUS and ANSYS performed as a reliable technique for empirical data validation and response prediction. In this case, the ABAQUS program has been numerically predicted the failure loads. Thus, comparing of results which are computed through FE model has shown a good agreement with test results, confirming that the length and discontinuous welding fillet for empty stubs has a drastic influence on load carrying capacity and the failure mode is majorly a premature local buckling mode. Thin-walled structures have demonstrated a sustainable strength against the axial compressive loads (Heydari *et al.* 2018, Taheri *et al.* 2019) and low flexural capacity, thermal stability and hysteresis response especially when their section was perforated or partially opened (Shah *et al.* 2015, Shah *et al.* 2016a, Shah *et al.* 2016b, Shah *et al.* 2016c, Shariati *et al.* 2018). Rectangular steel tubs with continuous welding on mid-depth improve the load carrying capacity for both rectangular empty steel and composite tubs. CFT columns with continuous welding has a greater lateral stiffness and rupture strength compared to the CFT columns with discontinuous welding steel sections (Hosseinpour *et al.* 2018). Test results have shown that I-shaped steel stubs have greater compression load carrying capacity with a lower load decrement rate compared to the traditional rectangular steel stubs with a height over 200 mm. I-shaped composite stubs wouldn't reach to the unlimited strength

when the failure mode is by local buckling of steel flange, steel–concrete bond failure and concrete crushing. In case of lateral stiffeners or shear connectors, I-shaped composite reach higher failure loads (Xu *et al.* 2019). The structural features of square CFT stub columns by using cold formed thin steel plates have been studied by (Lee *et al.* 2011b). Concrete has outstanding compressive strength due to its dense and robust texture which does not experience the local or distortional buckling or other accidental deformations along with low flexural and torsional strength which made the concrete a useful material for columns axial structural elements (Nosrati *et al.* 2018, Shariati *et al.* 2019c, Trung *et al.* 2019a). Accordingly, thin walled cold-formed square column steel square concrete filled tubular column has been introduced and structural function of the welded built-up square stub column has been analyzed by the structural experiment for ten specimens with concrete strength's parameters, steel tube type, and the ratio of width to thickness in steel tube (Lee *et al.* 2011a). In both generic CFT specimens and welded built-up CFT specimens, out-of-plane local buckling has been observed at the edges of ribs set up for preventing the stress concentration in the lower and upper ends of columns followed by a steady increment in load capacity. Later, load capacity is progressively decreased when the column center swelled. Also, the composite effect of concrete and steel is improved by the vertical inner anchor. Since the ribs set up within the steel tubes of welded built-up square CFT columns reduce the width thickness rate, the load capacity of columns is increased. Columns with higher concrete strength have higher load bearing capacity, because concrete core delays the local buckling of steel tube. High strength steel could be applied to decline the local buckling and to use thinner steel tube (Lee *et al.* 2011a, Shariati *et al.* 2019d, Shariati *et al.* 2019e). A research by (Abed *et al.* 2013) has experimentally and numerically investigated the compressive behavior of circular Concrete Filled Steel Tubes (CFSTs) under axial compressive loads. It was found that B/t ratio has a greater effect on load bearing capacity of CFT columns compared to concrete strength. By increasing B/t ratio, axial strength and members' stiffness are decreased because steel tube has provided less confinement to concrete. Also, the column's ductility is decreased when the concrete infill strength is increased for higher D/t rates, but for lower D/t rate, the opposite is true. Few formulas and equations are verified to measure the axial capacity of CFST columns. Typically, many models have provided conservative estimates, except for the ones defined by (Mander *et al.* 1988b) who said that the deviations of estimates (test results) are reduced when D/t ratio is increased, which is attributed to the reduced confinement effects at high D/t ratios. FE model has been analyzed with one of the tested CFST samples after incorporating the material nonlinearity of steel tube and concrete infill. Test data and the output of model have shown a good agreement in terms of axial capacity and failure mode. Like the failure modes occurred in tested specimens. Dominant failure mode in FE analysis of CFST columns is local buckling of steel tube followed by the crushing of concrete infill. For the modeled CFST specimen, steel tube is bulged outwards locally near the loading ends and in the mid-height of specimens. The buckling at the mid-height of column took place at the early stages of loading time followed by a localized buckling near the ends of element. Similar failure modes have been occurred across the tests for all CFST specimens (Xu *et al.* 2019). In another research (Tao *et al.* 2005) has conducted a test on concrete-filled steel tubular stub columns with inner or outer welded longitudinal stiffeners under axial compression. The sectional capacity of the composite stub columns has been raised when stiffeners are provided. Thus, the longitudinal stiffeners could both delay the local buckling of the plate panel, and surpass the lateral curb of concrete core. The outer stiffened specimens have approximately represented the same behavior as the inner stiffened ones, however, the stiffeners should have higher flexural rigidities to ensure their effectiveness. The larger *D/t* ratio is, the larger the rigidity requirement of stiffeners is. Theoretical method and design codes have been applied for the prediction of load versus axial strain relationships and load-carrying capacities of the adequately stiffened composite sections that is followed by reasonable results. The mentioned design codes have generally underestimated the strength of adequately stiffened stub columns. By considering confinement enhancement effects from stiffeners, the prediction of load-carrying capacities of columns has been formulated (Ahmadi *et al.* 2017, Trung *et al.* 2019b). Regarding all the studies in welded built-up sections, few insights have been provided into the influence of various confinement steel tubes with various welding lines (stiffeners) on load capacity of CFT stub columns (Tao *et al.* 2005). The objective of this study is to study the axial performance of built-up CFT tube columns composed by connecting two pieces of cold-formed U-shaped or four pieces of L-shaped thin steel plates with continuous penetration groove welding line located at mid-depth of stub column section. High strength welding lines have been applied due to higher thickness and yield stress of welding lines compared to steel tubes. ABAQUS finite element is used to study the nonlinear performance of welded built-up CFT columns subjected to axial pressure (Systèmes 2007). In terms of key parameters of this study, two cross sectional types as U-shaped and L-shaped, compressive strength of filled concrete (C20, C40, and C80), and the effect of welding lines are provided.

2. FE model

Abaqus has been numerically measured the behavior and ultimate strength of Welded built-up steel box columns fabricated by connecting two pieces of cold-formed U-shaped or four pieces of L-shaped thin steel plates under axial pressure. Accordingly, actual elastic-plastic, non-linear materials, engineering considerations, and stress-strain relationship obtained from the test have been evaluate in numerical method. Typical static model has been used in the analytical model and loading is controlled by considering the displacement.

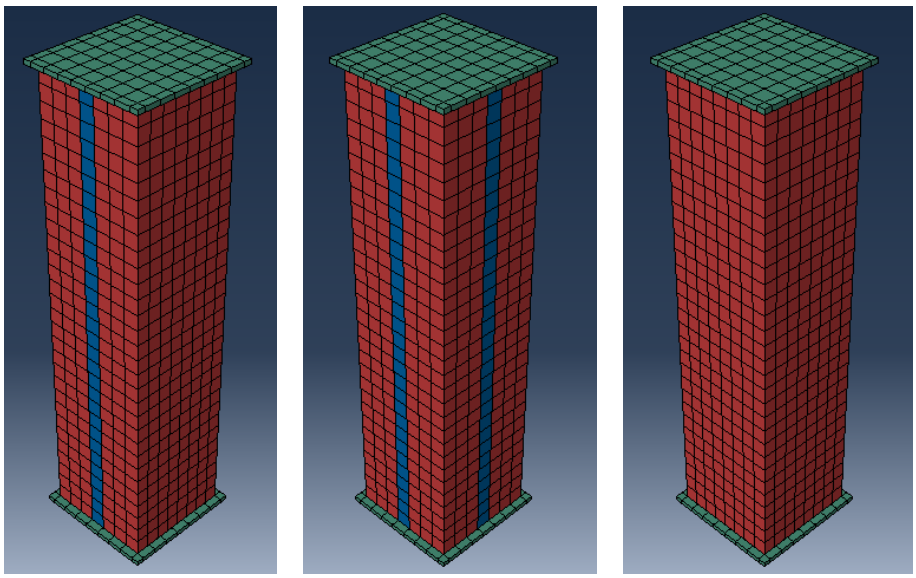

Fig. 3 Mesh types used in the numerical model (a) Numerical model without welding line, (b) Numerical model with 4 welding lines and (c) Numerical model with 2 welding lines

2.1 Element type and mesh

Four-node reduced shell (S4R) element has been used for modeling the steel tube and welding line including 6 degrees of freedom at each node as a precise resolution for many applications (Systèmes 2007, Sedghi *et al.* 2018). Moreover, eight nodes have reduced the solid element with 3 degrees of freedom at each node (C3D8R) used for the concrete core inside the steel tube (Fig. 3), also various mesh sizes are examined to gain reliable results with less computational cost.

2.2 Loading of the boundary element

Applied boundary conditions in FE model has reflected the prior test conditions in which two rigid plates have been simulated at the bottom and top of the specimens, representing the loading device and supporting the test model. RP is defined for each plate for which the boundary conditions have been applied so that the plates are fixed at all degree(s) of freedom except in a direction in which the displacement has been applied (axial loading to RP along the axis 3 is applied through displacement downwards).

2.3 Modelling of interaction between steel wall and filled concrete

The interaction between concrete and steel has been modeled through the contact pair option and choosing the surface to surface contact (Systèmes 2007, Sedghi *et al.* 2018a) in which two contact surfaces are required and called master and slave (to decline the numerical errors, the slave surface should be selected from a softer material and also have a better mesh than master surface). Afterwards, the internal surface of steel tube wall and the outer surface of concrete are identified as master and slave surfaces. The normal behavior between slave and master surfaces is simulated by "hard" contact which permits the separation of two surfaces after contact. On the other hand, tangent behavior between two surfaces is simulated by Coulomb friction model with a friction coefficient of 0.25.

2.4 Modeling of the confined concrete

Based on the literature, the concrete core in CFT columns has been limited by steel tubes and the confinement effect has been decreased by the raise of fy and B/t ratios, which should be considered in a concrete model that is simulated in Abacus model (Systèmes 2007, Lim *et al.* 2014). Fig. 4 represents the stress-strain curves of the confined and unconfined concrete. f_c and ε_c show the compressive strength and its corresponding strain in unconfined concrete (Safa *et al.* 2016, Trung *et al.* 2019a). Also f_{cc} and ε_0 are the stress and strain of the confined concrete. The strain correspondent to the stress in unconfined concrete is computed by use of Eq. (1) suggested by (Tasdemir *et al.* 1998).

The ultimate strength of confined concrete and its correspondent strain can be expressed as Eqs. (2) and (3), in which Eq. (2) has been suggested by Xiao et al and used for numerical modeling of normal and high strength concrete (Xiao *et al.* 2010, Taheri *et al.* 2019), also Eq. (3) is proposed by (Lim and Ozbakkaloglu 2014).

In the Eq. (3), f_r and f_c' are in MPais calculated by ε_c Eq. (1). f_{re} is the residual stress of confined, concrete and calculated by Eq. (4). The inflection point (ec,i) of descending branch is computed by Eq. (5).

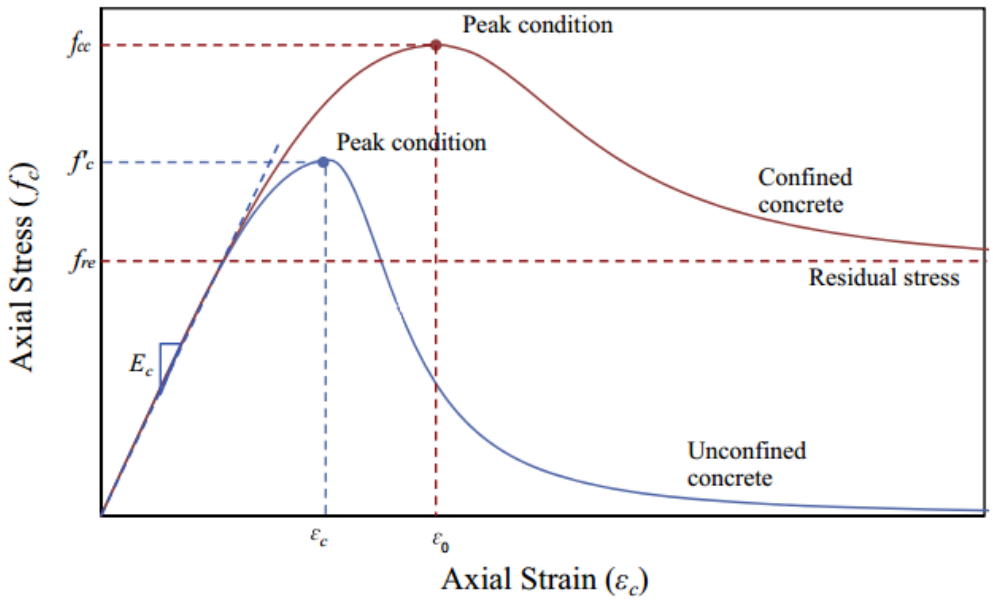

Fig. 4 Stress-strain curves of unconfined and confined concrete (Lim *et al*. 2014)

In the Eq. (5), the post peak region of the confined concrete curve was plotted using the proposed stress-axial strain equation by (Popovics 1973),which was then modified by (Mander *et al.* 1988a). In this equation f_{cc} , f_r and f_c are in MPa. and $\rho_{c,f}$ is in kg/m^3 .

The plastic model of concrete failure in Abaqus has been used in numerical modeling of concrete core. Thus, the default variables of 0.1 and 0 are applied for the flow potential eccentricity and viscosity parameter. All other parameters of this concrete like dilation angle ψ, $\frac{f_{b0}}{f_c}$ ratio an k_c can be determined by the Eqs. (10) to (12) recommended by (Tao *et al.* 2005).

$$\varepsilon_c = (-0.067 f_c'^2 + 29.9 f_c' + 1055) * 10^{-6} \quad (1)$$

$$\frac{f_{cc}}{f_c'} = 1 + 3.24\left(\frac{f_r}{f_c'}\right)^{0.8} \quad (2)$$

$$\varepsilon_0 = \varepsilon_c + 0.045\left(\frac{f_r}{f_c'}\right)^{1.15} \quad (3)$$

$$f_{re} = 1.6 f_{cc}\left(\frac{f_r^{\,0.24}}{f_c^{\,0.32}}\right) \quad \dots f_{re} \le f_{cc} - 0.15 f_c' \quad (4)$$

$$\varepsilon_{c,i} = (2.8\varepsilon_{cc}\left(\frac{f_{re}}{f_{cc}}\right) f_c'^{-0.12} + 10\varepsilon_{cc}(1 - \frac{f_{re}}{f_{cc}}) f_c'^{-0.47})(\frac{\rho_{c,f}}{2400})^{0.4} \quad (5)$$

$$f_c = f_{cc} - \frac{f_{cc} - f_{re}}{1 + \left(\frac{\varepsilon_c - \varepsilon_0}{\varepsilon_{c,i} - \varepsilon_0}\right)^{-2}} \quad (6)$$

In Eq. (6), the pre peak region of confined concrete curve has been modeled by (Binici 2005, Usefi *et al.* 2019)

$$f = f_{re} + (f_c' + f_{re}) \exp\left[-\left(\frac{\varepsilon - \varepsilon_0}{\alpha}\right)^{\beta}\right] \quad (7)$$

β= equal to 0.92
α= proposed by (Tao *et al.* 2005)

$$\alpha = 0.005 + 0.0075\xi \quad (8)$$

ξ = Confinement coefficient of CFT columns presented in Eq. (7)

$$\xi = \frac{A_s f_y}{A_c f_c} \quad (9)$$

As and A_s = the area of steel and concrete

$$\psi = 40^0 \quad (10)$$

$$\frac{f_{b0}}{f_c} = \frac{1.5}{f_c^{\,0.075}} \quad (11)$$

$$k_c = \frac{5.5}{5 + 2 f_c^{\,0.075}} \quad (12)$$

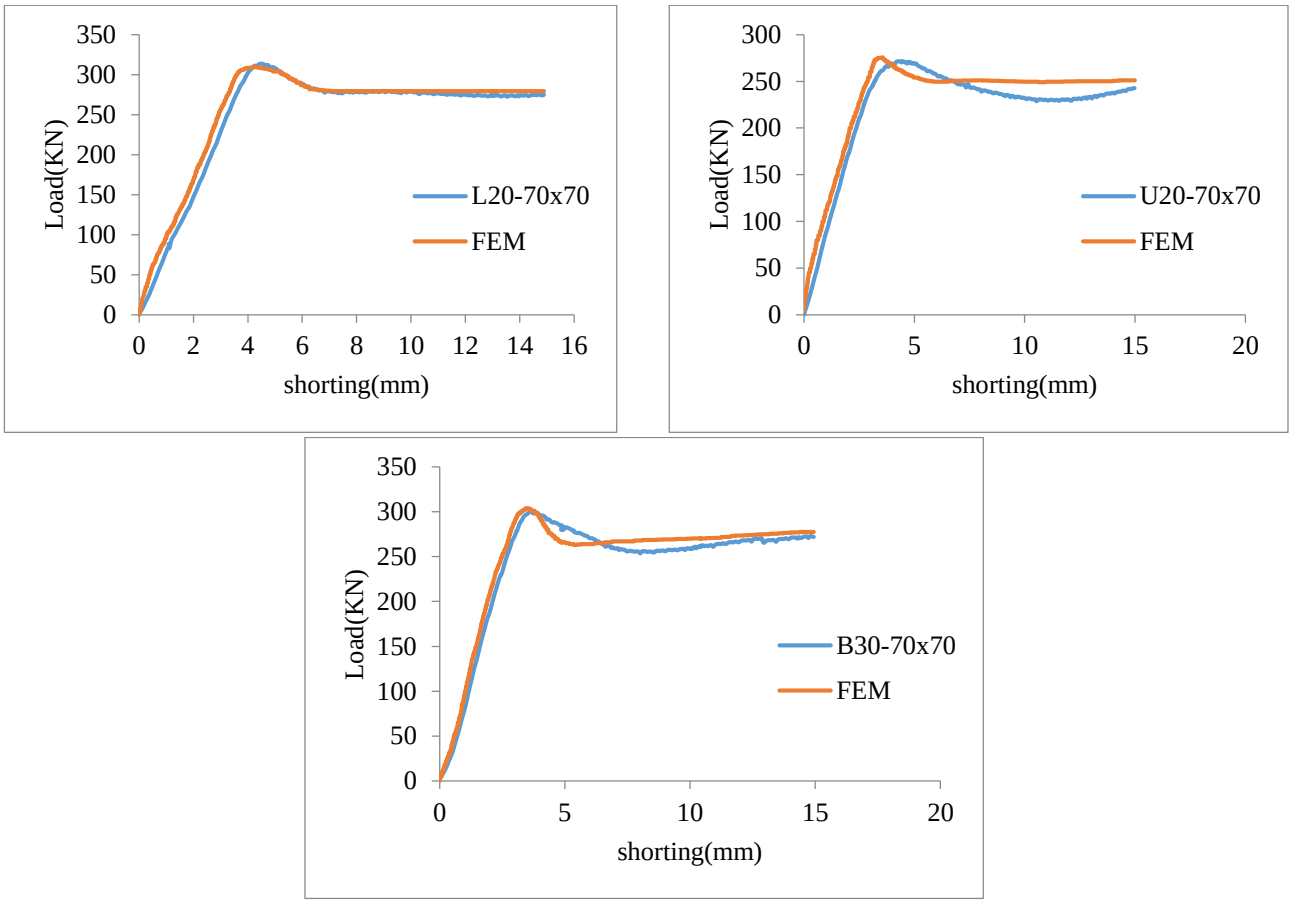

Fig. 5 Comparison of numerical and experimental results (Sharafi *et al.* 2018a)

2.5 Model verification

To verify the numerical modeling, the results have been compared to the test results of force-displacement, thus the numerical results are in a good agreement with test results (Fig. 5) (Sharafi *et al.* 2018a).

According to Fig. 6, simulated buckling is similar to the experimental buckling. Therefore, comparing of results has shown an acceptable ability of FE in simulating other parameters which has not been investigated in an experimental study.

3. Numerical simulation and discussion

In this section, the results of nonlinear analyses of short built-up CFT columns composed with steel plates are presented. In order to prepare welded built-up specimens, steel boxes are fabricated by connecting of four pieces of L-shaped thin steel plates or two pieces of cold-formed U-shaped (Fig. 7).

The models are grouped in terms of different cross sections and concrete strength:

1. Generic CFT columns with no welding lines (B specimens)
2. Built-up CFT columns with 2 welding lines (U specimens)
3. Built-up CFT columns with 4 welding lines (L specimens)

The nomenclature used in this section (B70×70-4-20, U70×70-4-20, L70×70-4-20) consists of a cross-sectional type in which "B" shows a column with no welding lines, "U" and "L" show columns with two pieces of cold-formed U-shaped and four pieces of L-shaped thin steel plates. The 1th and 2nd number show the cross sectional dimensions, also the steel tube wall thickness and compressive strength of concrete are shown by the 3rd and 4th number. The load-displacement curves under axial compression for CFT columns with no welding lines in terms of different B/t ratios and concrete strength (20,40, and 80) are shown in Fig. 8. Therefore, B/t ratio is increased by the load bearing capacity increment. More ductile behavior compared to others because of lower concrete strength is shown in Fig. 8(a). Furthermore, these specimens have similar descending and ascending rate. However, the descending branch rate for specimen in Fig. 8(c) has been significantly changed due to greater concrete strength. Also, by the raise of steel tube thickness, the load bearing capacity has been also increased due to more confinement effect. Respectively, the average raising ratio is 16% and 35% for B120×120 and B70×70 specimens, deduced that for a greater cross section, the raise of concrete strength has led to higher load bearing capacity compared to the raise of steel tube thickness. In contrast, the reverse case is true for columns with lower sizes. Moreover, higher concrete strength leads to higher load bearing capacity.

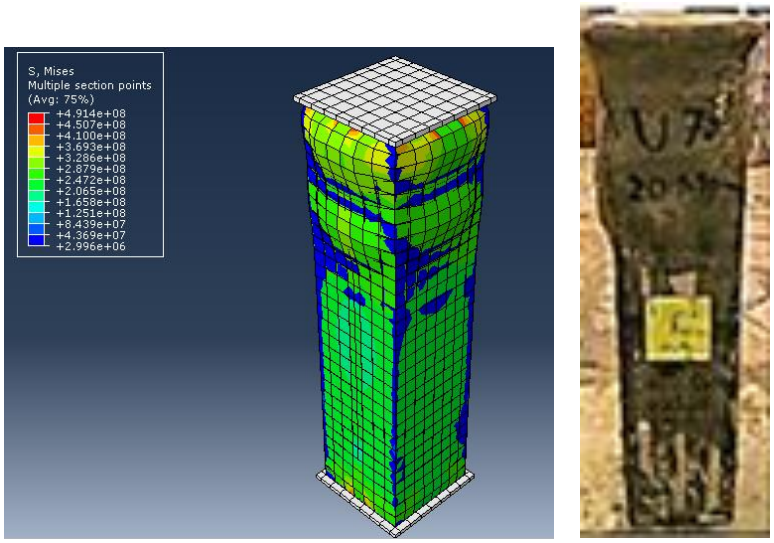
S, Mises
Multiple section points
(Avg: 75%)
+4.914e+08
+4.507e+08
+4.100e+08
+3.693e+08
+3.286e+08
+2.879e+08
+2.472e+08
+2.065e+08
+1.658e+08
+1.251e+08
+8.439e+07
+4.369e+07
+2.996e+06

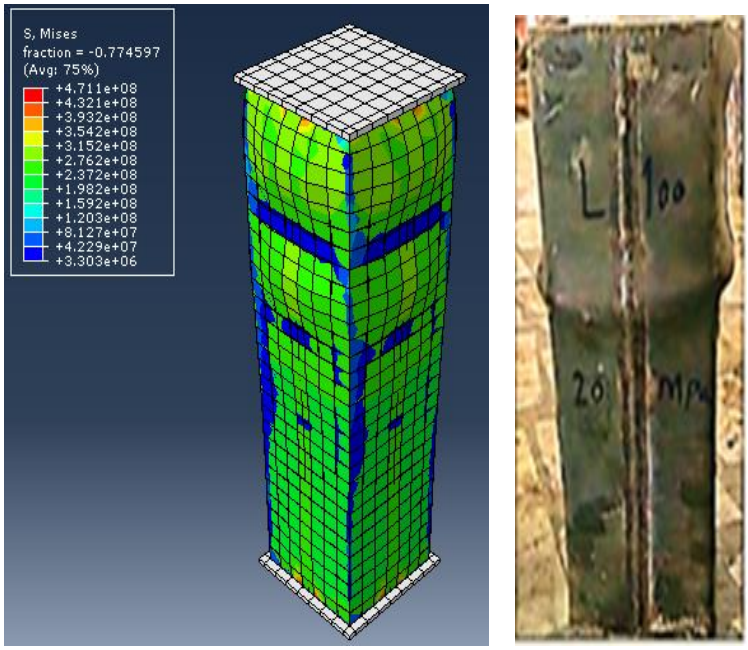
S, Mises
fraction = -0.774597
(Avg: 75%)
+4.711e+08
+4.321e+08
+3.932e+08
+3.542e+08
+3.152e+08
+2.762e+08
+2.372e+08
+1.982e+08
+1.592e+08
+1.203e+08
+8.127e+07
+4.229e+07
+3.303e+06

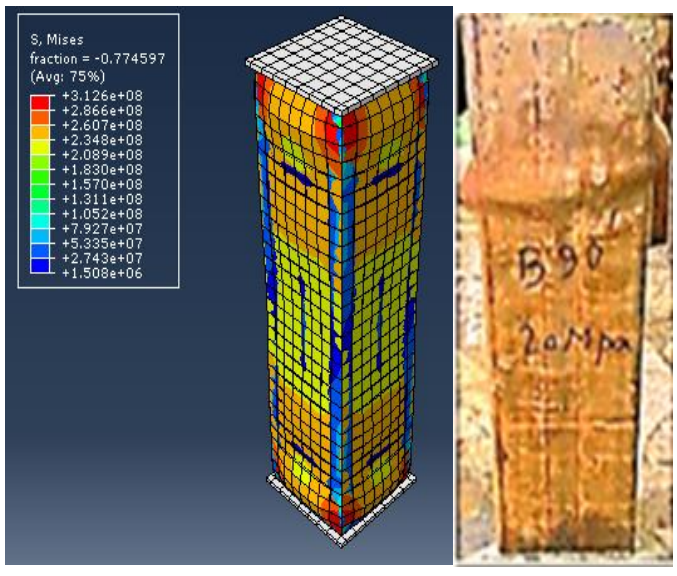
S, Mises
fraction = -0.774597
(Avg: 75%)
+3.126e+08
+2.866e+08
+2.607e+08
+2.348e+08
+2.089e+08
+1.830e+08
+1.570e+08
+1.311e+08
+1.052e+08
+7.927e+07
+5.335e+07
+2.743e+07
+1.508e+06

Continued-

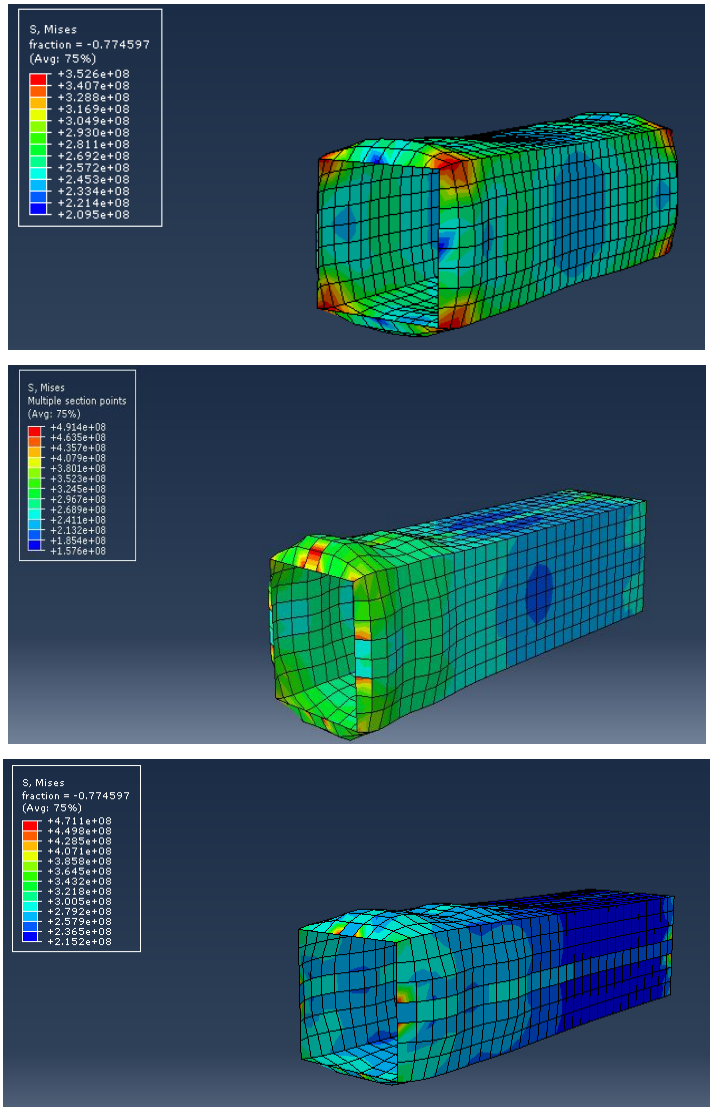

Fig. 6 Comparing of failure in experimental (Sharafi *et al.* 2018a) and numerical models for cold-formed CFT columns

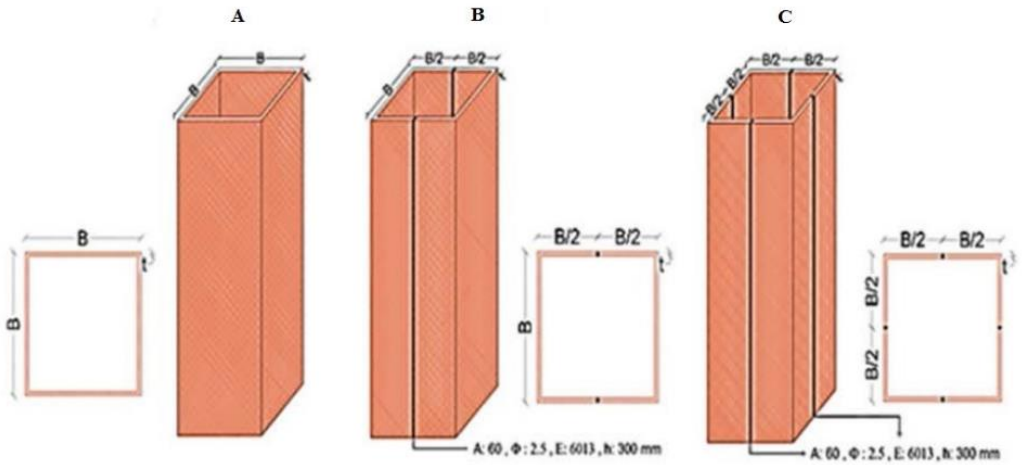

Fig. 7 (a) Generic Steel box section, (b) Steel box made by connecting two pieces of cold-formed U-shaped steel plates, and (c) Steel box made by connecting four pieces of cold-formed L-shaped steel plates

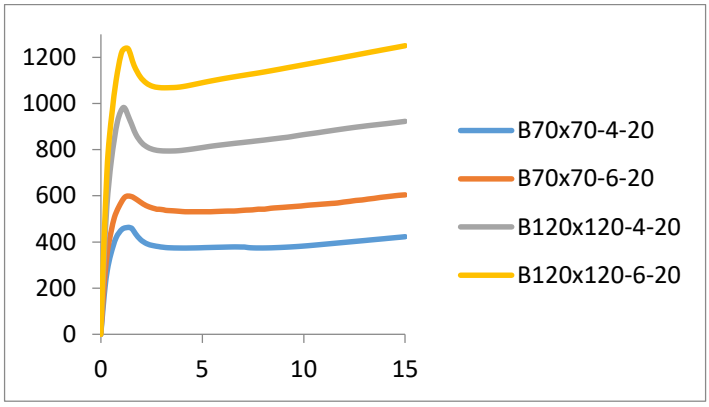

(a)

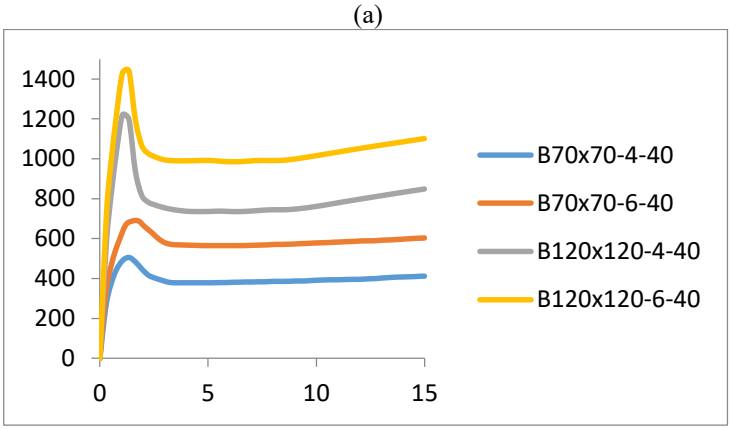

(b)

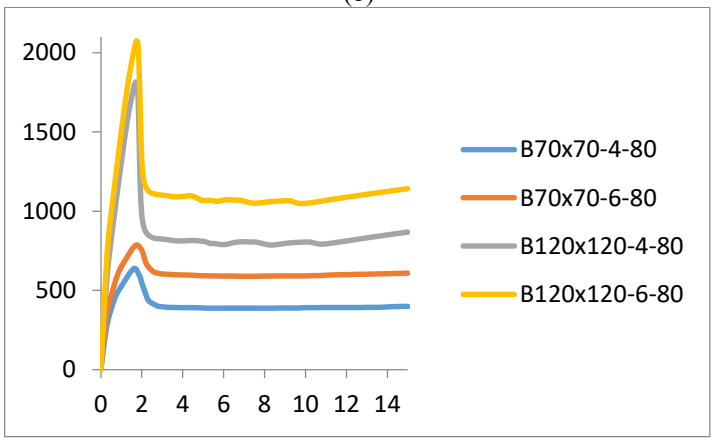

(c)

Fig. 8 Load-displacement curves of columns with no welding lines (a) Compressive strength is 20 MPa, (b) Compressive strength is 40 MPa and (c) Compressive strength is 80 MPa

Apparently, in CFT columns with higher cross section, the influence of concrete strength on load bearing capacity is more visible. The load bearing capacity of B120×120-6-80 increased by 42% is compared to B120×120-6-40 and 16% for B120×120-6-40 is compared to B120×120-6-20. However, B 70×70-6-80 with an increment of 13% is compared to B 70×70-6-40 and B 70×70-6-40 with an increment by 7% is compared to B 70×70-6-20. As a result, for greater cross section, the raise of concrete strength has led to higher load bearing capacity which is compared to the raise of steel tube thickness. In contrast, the reverse is true for columns with lower sizes.

Fig. 9 shows the load-displacement curves under axial compression for built-up CFT columns with 2 welding lines (U specimens) considering different B/t ratios and concrete strength (20, 40.80). Thus, in CFT columns with higher cross section, concrete strength has a significant effect on load bearing capacity. U120×120-6-80 with an increment of 47% is compared to U120×120-6-40 and U120×120-6-40 with an increment by 25% is compared to U120×120-6-20. This finding is more noticeable than CFT columns with no welding lines. U70×70-6-80 with an increment by 29% is compared to U70×70-6-40 and U70×70-6-40 with an increment of 3% is compared to U70×70-6-20. This is due

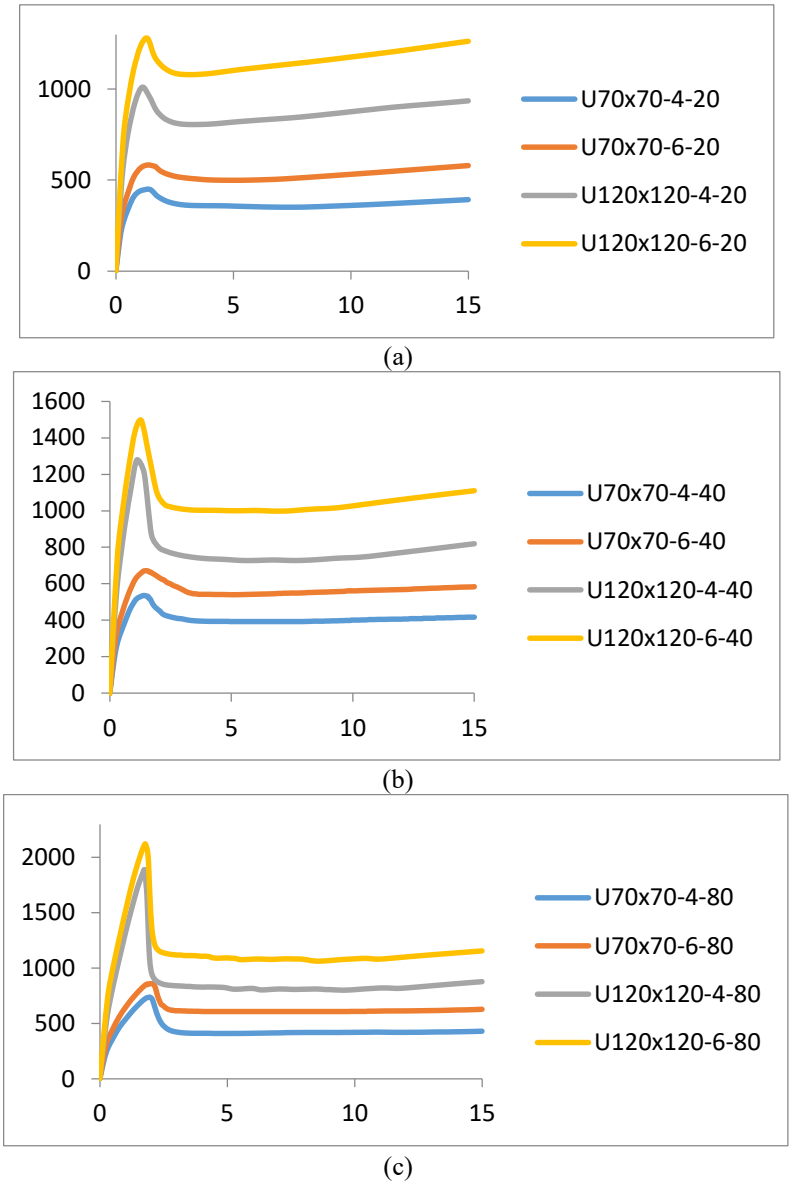

Fig. 9 Load-displacement curves of columns with two welding lines. (a) Compressive strength is 20 MPa, (b) Compressive strength is 40 MPa and (c) Compressive strength is 80 MPa

to the fact that columns with two welding lines (stiffeners) can provide more confinement effect. Additionally, the load bearing capacity of these specimens has been increased when the steel tube thickness is increased due to more confinement effect, representing an average increment of 21% and 40% for U120×120 and U70×70, respectively. For greater cross section, an increment of concrete strength has resulted a higher load bearing capacity compared to the increment of steel tube thickness. However, the reverse is true for columns with lower sizes. Moreover, higher concrete strength has higher load bearing capacity. Thereafter, columns with lower concrete strength have shown more ductile behavior compared to others. Moreover, speeding rate for columns in 6a is roughly the same as both ascending and descending branch.

However, descending branch for specimens in 6c has been significantly changed at higher rate. Also, when B/t ratio is decreased the load bearing capacity is increased.

The load-displacement curves under axial compression for CFT columns with four welding lines with different B/t ratios and concrete strength (20, 40, and 80) is shown in Fig. 10.

Accordingly, B/t ratio is increased by the load bearing capacity increment. In CFT columns with higher cross section, concrete strength has a greater impact on load bearing capacity. The load bearing capacity of L120×120-6-80 increased by 51% is compared to L120×120-6-40 and the load bearing capacity of L120×120-6-40 increased by 23% is compared to L120×120-6-20. Also, L70×70-6-80 with an increment of 31% is compared to L70×70-6-40, and L70×70-6-40 with an increment of 16% is compared to L70×70-6-20. Therefore, columns with four welding lines (stiffeners) have higher load bearing capacity compared to columns with two and no welding lines. Additionally, the load bearing capacity of these specimens is increased when the steel tube thickness is increased due to more

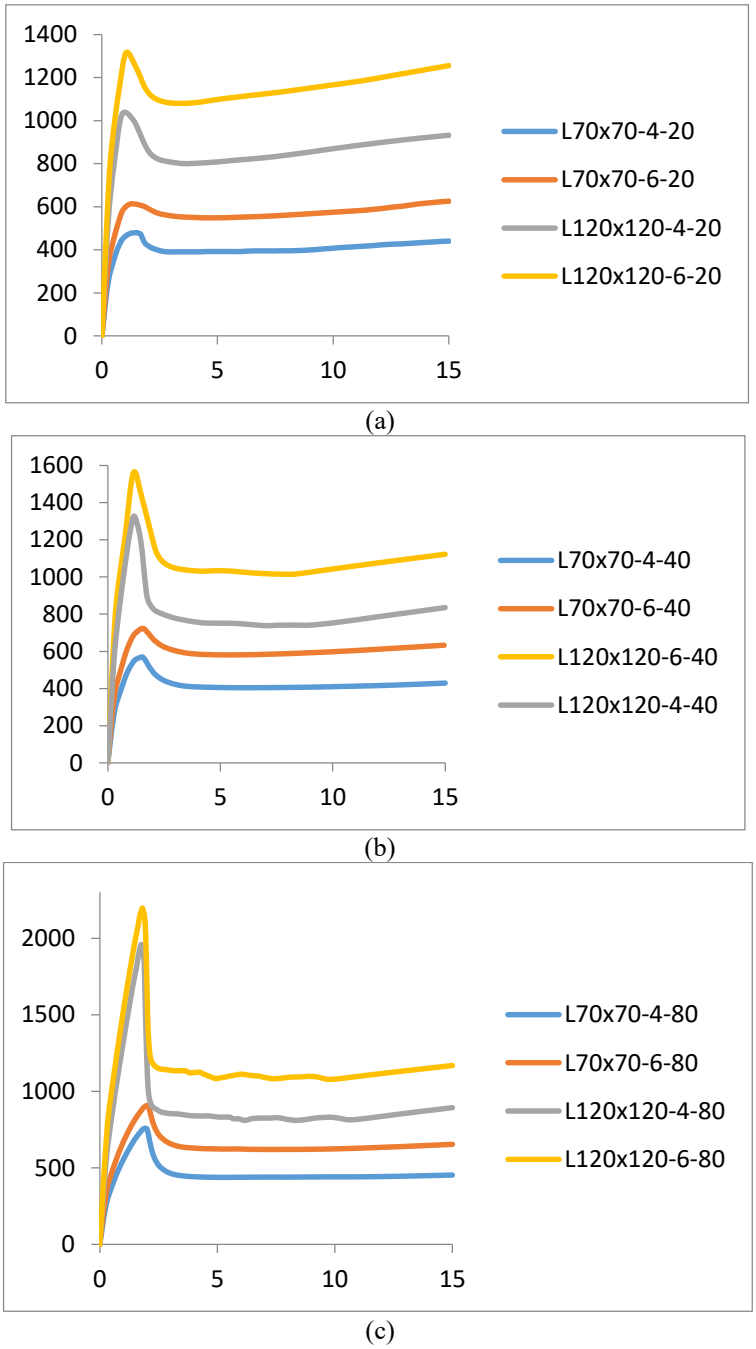

Fig. 10 load-displacement curves of columns with four welding lines. (a) Compressive strength is 20 MPa, (b) Compressive strength is 40 MPa and (c) Compressive strength is 80 MPa

confinement effect, with an average increment of 24.3% and 40% for L120×120 and L70×70, respectively. Alternatively, the increment of concrete strength with greater cross section has led to higher load bearing capacity compared to the increment of steel tube thickness. As a result, by the increment of steel tube thicknesses, the CFT columns with more welding lines have obtained the highest ultimate strength.

4. Conclusions

This study has presented a numerical model for the simulation of built-up concrete filled steel tube columns under axial pressure using the FE with ABAQUS. Subsequently, FE is validated by comparing axial load bearing capacity and typical failure patterns of steel tube and core concrete of corresponding experimental specimens. Consequently, the proposed model can be applied to predict the axial load capacity and local buckling of CFT columns.

- Welding lines (stiffeners) are effective on increasing the confining pressure of built-up CFT columns while they are increasing the confinement strength of concrete and raising the ductility and load bearing capacity of concrete.
- By raising the welding lines, the confining pressure has been also increased. However, by raising B/t ratio and concrete strength, the confining pressure has experienced a decrement.
- By the increment of steel tube thickness, the load bearing capacity of columns is raised due to more confinement effect. This average amount is more significant in CFT columns with more stiffeners.

Concrete strength increment with more cross section has led to higher load bearing capacity compared to the steel tube thickness increment.

- In CFT columns with greater cross section, concrete strength has greater influence on load bearing capacity, which is more noticeable in columns with four welding lines.
- A good agreement has been occurred between the numerical model and experimental outcomes while considering the failure state. Thus, the proposed numerical FE method could be properly applied for the subsequent parametric researches to scrutinize the other factors affecting CFT columns.

Acknowledgements

The research presented in this paper was supported by Babol Noshirvani University of Technology (Award No: BNUT934140052). The support is gratefully acknowledged.

References

Abed, F., AlHamaydeh, M. and Abdalla, S. (2013), "Experimental and numerical investigations of the compressive behavior of concrete filled steel tubes (CFSTs)", *J. Constr. Steel Res.*, **80**, 429-439. https://doi.org/10.1016/j.jcsr.2012.10.005.

Ahmadi, M., Naderpour, H. and Kheyroddin, A. (2019), "A proposed model for axial strength estimation of non-compact and slender square CFT columns", *Iran. J. Sci. Technol. T. Civil Eng.*, **43**(1), 131-147. https://doi.org/10.1016/j.jcsr.2012.10.015.

Ahmadi, M., Naderpour, H., Kheyroddin, A. and Gandomi, A.H. (2017), "Seismic failure probability and vulnerability assessment of steel-concrete composite structures", *Periodica Polytechnica Civil Eng.*, **61**(4), 939-950. https://doi.org/10.1015/j.jcsr.2012.10.005.

Ahmadi, R., Rashidian, O., Abbasnia, R., Mohajeri Nav, F. and Usefi, N. (2016), "Experimental and numerical evaluation of progressive collapse behavior in scaled RC beam-column subassemblage", *Shock Vib.*, https://doi.org/10.1155/2016/3748435.

Arabnejad Khanouki, M., Ramli Sulong, N. and Shariati, M. (2010), "Investigation of seismic behaviour of composite structures with concrete filled square steel tubular (CFSST) column by push-over and time-history analyses", *Proceedings of the 4th International Conference on Steel & Composite Structures*.

Arabnejad Khanouki, M.M., Ramli Sulong, N.H. and Shariati, M. (2011), "Behavior of through beam connections composed of CFSST columns and steel beams by finite element studying", *Adv. Mater. Res.*, **168**, 2329-2333. DOI: 10.1016/j.jcsr.2011.01.002.

Arabnejad Khanouki, M.M., Ramli Sulong, N.H., Shariati, M. and Tahir, M.M. (2016), "Investigation of through beam connection to concrete filled circular steel tube (CFCST) column", *J. Constr. Steel Res.*, **121**, 144-162. DOI: 10.1016/j.jcsr.2016.01.002.

Binici, B. (2005), "An analytical model for stress–strain behavior of confined concrete", *Eng. Struct.*, **27**(7), 1040-1051. DOI: 10.1016/j.engstruct.2005.03.002.

Chen, C., Shi, L., Shariati, M., Toghroli, A., Mohamad, E.T., Bui, D. T. and Khorami, M. (2019), "Behavior of steel storage pallet racking connection-A review.", *Steel Compos. Struct.*, **30**(5), 457-469. https://doi.org/10.12989/scs.2019.30.5.457.

Daie, M., Jalali, A., Suhatril, M., Shariati, M., Arabnejad Khanouki, M.M., Shariati, A. and Kazemi Arbat, P. (2011), ""A new finite element investigation on pre-bent steel strips as damper for vibration control", *Int. J. Phys. Sci.*, **6**(36), 8044-8050. https://doi.org/10.5897/IJPS11.1585.

Davoodnabi, S.M., Mirhosseini, S.M. and Shariati, M. (2019), "Behavior of steel-concrete composite beam using angle shear connectors at fire condition", *Steel Compos. Struct.*, **30**(2), 141-147. https://doi.org/10.12989/scs.2019.30.2.141.

Gupta, P.K., Ahuja, A.K. and Khaudhair, Z.A. (2014), "Modelling, verification and investigation of behavior of circular CFST columns", *Struct. Concrete*, **15**(3), 340-349. https://doi.org/10.1002/suco.201300045.

Han, L.H., Li, W. and Bjorhovde, R. (2014), "Developments and advanced applications of concrete-filled steel tubular (CFST) structures: Members", *J. Constr. Steel Res.*, **100**, 211-228. https://doi.org/10.1016/j.jcsr.2014.04.016.

Heydari, A. and Shariati, M. (2018), "Buckling analysis of tapered BDFGM nano-beam under variable axial compression resting on elastic medium", *Struct. Eng. Mech.*, **66**(6), 737-748. https://doi.org/10.12989/sem.2018.66.6.737.

Hosseinpour, E., Baharom, S., Badaruzzaman, W.H.W., Shariati, M. and Jalali, A. (2018), "Direct shear behavior of concrete filled hollow steel tube shear connector for slim-floor steel beams", *Steel Compos. Struct.*, **26**(4), 485-499. https://doi.org/10.12989/scs.2018.26.4.485.

Ismail, M., Shariati, M., Abdul Awal, A.S.M., Chiong, C.E., Sadeghipour Chahnasir, E., Porbar, A., Heydari, A. and khorami, M. (2018), "Strengthening of bolted shear joints in industrialized ferrocement construction", *Steel Compos. Struct.*, **28**(6), 681-690. https://doi.org/10.12989/scs.2018.28.6.681.

Jalali, A., Daie, M., Nazhadan, S.V.M., Kazemi-Arbat, P. and Shariati, M. (2012), "Seismic performance of structures with pre-bent strips as a damper", *Int. J. Phys. Sci.*, **7**(26), 4061-4072. DOI: 10.5897/IJPS11.1324.

Jalali, A., Toghroli, A., Shariati, M. and Ibrahim, Z. (2017), "Assessment of stiffened angle shear connector under monotonic and fully reversed cyclic loading", *Proceedings of the 5th International Conference on Advances in Civil, Structural and Mechanical Engineering - CSM 2017, Institute of Research Engineers and Doctors*.

Judd, J.P. and Pakwan, N. (2018), "Seismic performance of steel moment frame office buildings with square concrete-filled steel tube gravity columns", *Eng. Struct.*, **172**, 41-54. https://doi.org/10.1016/j.engstruct.2018.06.016.

Katebi, J., Shoaei-parchin, M., Shariati, M., Trung, N.T. and Khorami, M. (2019), "Developed comparative analysis of metaheuristic optimization algorithms for optimal active control of structures", Engineering with Computers, 1-20.

Khorami, M., Alvansazyazdi, M., Shariati, M., Zandi, Y., Jalali, A. and Tahir, M. (2017a), "Seismic performance evaluation of buckling restrained braced frames (BRBF) using incremental nonlinear dynamic analysis method (IDA)", http://dx.doi.org/10.12989/eas.2017.13.6.531.

Khorami, M., Khorami, M., Motahar, H., Alvansazyazdi, M., Shariati, M., Jalali, A. and Tahir, M. (2017b), "Evaluation of the seismic performance of special moment frames using incremental nonlinear dynamic analysis", *Struct. Eng. Mech*., **63**(2), 259-268. https://doi.org/10.12989/sem.2017.63.2.259.

Khorramian, K., Maleki, S., Shariati, M. and Ramli Sulong, N.H. (2015), "Behavior of tilted angle shear connectors", *PLoS One*, **10**(12), e0144288. DOI: 10.1371/journal.pone.0144288.

Khorramian, K., Maleki, S., Shariati, M., Jalali, A. and Tahir, M. (2017), "Numerical analysis of tilted angle shear connectors in steel-concrete composite systems", *Steel Compos. Struct*., **23**(1), 67-85. https://doi.org/ 10.12989/scs.2017.23.1.067.

Kildashti, K., Samali, B., Mortazavi, M., Ronagh, H. and Sharafi, P. (2019), "Seismic collapse assessment of a hybrid cold-formed hot-rolled steel building", *J. Constr. Steel Res.*, **155**, 504-516. https://doi.org/10.1016/j.jcsr.2019.01.010.

Lee, S.H., Kim, S.H., Bang, J.S., Won, Y.A. and Choi, S.M. (2011b), "Structural characteristics of welded built-up square concrete filled tubular stub columns associated with concrete strength", *Procedia Eng*., **14**, 1140-1148. https://doi.org/10.1016/j.proeng.2011.07.143.

Lim, J.C. and Ozbakkaloglu, T. (2014), "Stress–strain model for normal-and light-weight concretes under uniaxial and triaxial compression", *Constr. Build. Mater.*, **71**, 492-509. https://doi.org/10.1016/j.conbuildmat.2014.08.050.

Luo, Z., Sinaei, H., Ibrahim, Z., Shariati, M., Jumaat, Z., Wakil, K., Pham, B.T., Mohamad, E.T. and Khorami, M. (2019), "Computational and experimental analysis of beam to column joints reinforced with CFRP plates", *Steel Compos. Struct.*, **30**(3), 271-280. http://dx.doi.org/10.12989/scs.2019.30.3.271.

Mander, J.B., Priestley, M.J.N. and Park, R. (1988b), "Theoretical stress-strain model for confined concrete", *J. Struct. Eng*., **114**(8), 1804-1826. DOI: 10.1061/(ASCE)0733-9445(1988)114:8(1804).

Mohammadhassani, M., Akib, S., Shariati, M., Suhatril, M. and Arabnejad Khanouki, M.M. (2014), "An experimental study on the failure modes of high strength concrete beams with particular references to variation of the tensile reinforcement ratio", *Eng. Fail. Anal*., **41**, 73-80. DOI: 10.1016/j.engfailanal.2013.08.014.

Mortazavi, M., Sharafi, P., Kildashti, K. and Samali, B. (2020), "Prefabricated hybrid steel wall panels for mid-rise construction in seismic regions", *J. Build. Eng*., **27**, 100942.

Nasrollahi, S., Maleki, S., Shariati, M., Marto, A. and Khorami, M. (2018), "Investigation of pipe shear connectors using push out test", *Steel Compos. Struct.*, **27**(5), 537-543. https://doi.org/10.12989/scs.2018.27.5.537.

Nosrati, A., Zandi, Y., Shariati, M., Khademi, K., Aliabad, M.D., Marto, A., Mu'azu, M., Ghanbari, E., Mandizadeh, M. and Shariati, A. (2018), "Portland cement structure and its major oxides and fineness", *Smart Struct. Syst*., **22**(4), 425-432. https://doi.org/10.12989/sss.2018.22.4.425.

Paknahad, M., Shariati, M., Sedghi, Y., Bazzaz, M. and Khorami, M. (2018), "Shear capacity equation for channel shear connectors in steel-concrete composite beams", *Steel Compos. Struct*., **28**(4), 483-494. https://doi.org/10.12989/scs.2018.28.4.483.

Popovics, S. (1973), "A numerical approach to the complete stress-strain curve of concrete", *Cement Concrete Res*., **3**(5), 583-599.

Sadeghipour Chahnasir, E., Zandi, Y., Shariati, M., Dehghani, E., Toghroli, A., Mohamed, E.T., Shariati, A., Safa, M., Wakil, K. and Khorami, M. (2018), "Application of support vector machine with firefly algorithm for investigation of the factors affecting the shear strength of angle shear connectors", *Smart Struct. Syst*., **22**(4), 413-424. http://dx.doi.org/10.12989/sss.2018.22.4.413.

Safa, M., Shariati, M., Ibrahim, Z., Toghroli, A., Baharom, S.B., Nor, N.M. and Petkovic, D. (2016), "Potential of adaptive neuro fuzzy inference system for evaluating the factors affecting steel-concrete composite beam's shear strength", *Steel Compos. Struct*., **21**(3), 679-688. http://dx.doi.org/10.12989/scs.2016.21.3.679.

Sajedi, F. and Shariati, M. (2019), "Behavior study of NC and HSC RCCs confined by GRP casing and CFRP wrapping", *Steel Compos. Struct*., **30**(5), 417-432. https://doi.org/10.12989/scs.2019.30.5.417.

Sedghi, Y., Zandi, Y., Shariati, M., Ahmadi, E., Azar, V.M., Toghroli, A., Safa, M., Mohamad, E.T., Khorami, M. and Wakil, K. (2018a), "Application of ANFIS technique on performance of C and L shaped angle shear connectors", *Smart Struct. Syst*., **22**(3), 335-340. https://doi.org/1012989/SSS.2018.22.3.335.

Shah, S., Sulong, N.R., Jumaat, M. and Shariati, M. (2016a), "State-of-the-art review on the design and performance of steel pallet rack connections", *Eng. Fail. Anal*., **66**, 240-258.

Shah, S., Sulong, N.R., Shariati, M. and Jumaat, M. (2015), "Steel rack connections: Identification of most influential factors and a comparison of stiffness design methods", *PloS One*, **10(**10), e0139422.

Shah, S., Sulong, N.R., Shariati, M., Khan, R. and Jumaat, M. (2016b), "Behavior of steel pallet rack beam-to-column connections at elevated temperatures", *Thin-Wall. Struct.*, **106**, 471-483.

Shah, S.N.R., Ramli Sulong, N.H., Khan, R., Jumaat, M.Z. and Shariati, M. (2016c), "Behavior of industrial steel rack connections", *Mech. Syst. Signal Pr*., **70-71**, 725-740.DOI: 10.1016/j.ymssp.2015.08.026.

Shao, Z. and Vesel, A. (2015), "Modeling the packing coloring problem of graphs", *Appl. Math. Model*., **39**(13), 3588-3595.

Sharafi, P., Mortazavi, M., Usefi, N., Kildashti, K., Ronagh, H. and Samali, B. (2018a), "Lateral force resisting systems in lightweight steel frames: recent research advances", *Thin-Wall. Struct*., **130**, 231-253.

Sharafi, P., Rashidi, M., Mortazavi, M., Samali, B. and Ronagh, H. (2018b), "Identification of factors and multi-criteria decision analysis of the level of modularization in building construction", *ASCE J. Archit. Eng*., 24.

Sharafi, P., Rashidi, M., Samali, B., Ronagh, H. and Mortazavi, M. (2018c), "Identification of factors and decision analysis of the level of modularization in building construction", *J. Architect. Eng*., **24**(2), 04018010. DOI: 10.1061/(ASCE)AE.1943-5568.0000313.

Shariat, M., Shariati, M., Madadi, A. and Wakil, K. (2018), "Computational lagrangian multiplier method by using for optimization and sensitivity analysis of rectangular reinforced concrete beams", *Steel Compos. Struct*., **29**(2), 243-256. https://doi.org/10.12989/scs.2018.29.2.243.

Shariati, A., Ramli Sulong, N.H., Suhatril, M. and Shariati, M. (2012a), "Investigation of channel shear connectors for composite concrete and steel T-beam", *Int. J. Phys. Sci*., **7**(11), 1828-1831.

Shariati, A., Shariati, M., Sulong, N.R., Suhatril, M., Khanouki, M. A. and Mahoutian, M. (2014a), "Experimental assessment of angle shear connectors under monotonic and fully reversed cyclic loading in high strength concrete", *Constr. Build. Mater*., **52**, 276-283.

Shariati, M. (2013), Behaviour of C-shaped Shear Connectors in Stell Concrete Composite Beams, Jabatan Kejuruteraan Awam, Fakulti Kejuruteraan, Universiti Malaya.

Shariati, M., Safaei Faegh, S., Mehrabi, P., Bahavarnia, S., Zandi, Y., Rezaee Masoom, D., Toghroli, A., Trung, N.T. and Salih, M.N. (2019), "Numerical study on the structural performance of corrugated low yield point steel plate shear walls with circular openings", *Steel Compos. Struct.*, **33**(4), 569-581. https://doi.org/10.12989/scs.2019.33.4.569.

Shariati, M., Mafipour, M. S., Mehrabi, P., Zandi, Y., Dehghani, D., Bahadori, A., Shariati, A., Trung, N. T., Salih, M.N. and Poi-Ngian, S. (2019b), "Application of extreme learning machine (ELM) and genetic programming (GP) to design steel-concrete composite floor systems at elevated temperatures", *Steel Compos. Struct*., **33**(3), 319. https://doi.org/10.12989/scs.2019.33.3.319

Shariati, M., Mafipour, M.S., Mehrabi, P., Bahadori, A., Zandi, Y., Salih, M.N.A., Nguyen, H., Dou, J., Song, X. and Poi-Ngian, S. (2019a), "Application of a hybrid artificial neural network-particle swarm optimization (ANN-PSO) model in behavior prediction of channel shear connectors embedded in Normal and high-strength concrete", *Appl. Sci*., **9**(24), 5534.

Shariati, M., Mafipour, M.S., Mehrabi, P., Shariati, A., Toghroli, A., Trung, N.T. and Salih, M.N.A. (2020), "A novel approach to predict shear strength of tilted angle connectors using artificial intelligence techniques", *Engineering with Computers*, 1-21. DOI: 10.1007/s00366-019-00930-x.

Shariati, M., Mafipour, M.S., Haido, J.H., Yousif, S.T., Toghroli, A., Trung, N.T. and Shariati, A. (2020a), "Identification of the most influencing parameters on the properties of corroded concrete beams using an Adaptive Neuro-Fuzzy Inference System (ANFIS)", *Steel Compos. Struct*., **34**(1), 155-170. DOI: https://doi.org/10.12989/scs.2020.34.1.155.

Shariati, M., Rafie, S., Zandi, Y., Fooladvand, R., Gharehaghaj, B., Mehrabi, P., Shariat, A., Trung, N.T., Salih, M.N. and Poi-Ngian, S. (2019c), "Experimental investigation on the effect of cementitious materials on fresh and mechanical properties of self-consolidating concrete", *Adv. Concrete Constr*., **8**(3), 225-237. https://doi.org/10.12989/acc.2019.8.3.225.

Shariati, M., Ramli Sulong, N., Suhatril, M., Shariati, A., Arabnejad Khanouki, M. and Sinaei, H. (2012b), "Fatigue energy dissipation and failure analysis of channel shear connector embedded in the lightweight aggregate concrete in composite bridge girders", *Proceedings of the 5th International Conference on Engineering Failure Analysis*, 1-4 July 2012, Hilton Hotel, The Hague, The Netherlands.

Shariati, M., Ramli Sulong, N.H., Arabnejad Khanouki, M.M. and Shariati, A. (2011), "Experimental and numerical investigations of channel shear connectors in high strength concrete", *Proceedings of the 2011 World Congress on Advances in Structural Engineering and Mechanics (ASEM'11+)*, Seoul, South Korea.

Shariati, M., Ramli Sulong, N.H., Shariati, A. and Khanouki, M.A. (2015), "Behavior of V-shaped angle shear connectors: experimental and parametric study", *Mater. Struct*., **49**(9), 3909-3926. DOI: 10.1617/s11527-015-0762-8.

Shariati, M., Ramli Sulong, N.H., Shariati, A. and Kueh, A.B.H. (2016), "Comparative performance of channel and angle shear connectors in high strength concrete composites: An experimental study", *Constr. Build. Mater*., **120**, 382-392. DOI: 10.1016/j.conbuildmat.2016.05.102.

Shariati, M., Ramli Sulong, N.H., Suhatril, M., Shariati, A., Arabnejad Khanouki, M.M. and Sinaei, H. (2013a), "Comparison of behaviour between channel and angle shear connectors under monotonic and fully reversed cyclic loading", *Constr. Build. Mater*., **38**, 582-593. DOI: 10.1016/j.conbuildmat.2012.07.050.

Shariati, M., Shariati, A., Sulong, N.R., Suhatril, M. and Khanouki, M.A. (2014b), "Fatigue energy dissipation and failure analysis of angle shear connectors embedded in high strength concrete", *Eng. Fail. Anal.*, **41**, 124-134. https://doi.org/10.1016/j.engfailanal.2014.02.017.

Shariati, M., Sulong, N.R. and Khanouki, M.A. (2012c), "Experimental assessment of channel shear connectors under monotonic and fully reversed cyclic loading in high strength concrete", *Mater. Design*, **34**, 325-331. https://doi.org/10.1016/j.matdes.2011.08.008.

Shariati, M., Sulong, N.R., Suhatril, M., Shariati, A., Khanouki, M. A. and Sinaei, H. (2013b), "Comparison of behaviour between channel and angle shear connectors under monotonic and fully reversed cyclic loading", *Constr. Build. Mater*., **38**, 582-593.

Shariati, M., Tahir, M.M., Wee, T.C., Shah, S.N.R., Jalali, A., Abdullahi, M.A.M. and Khorami, M. (2018), "Experimental investigations on monotonic and cyclic behavior of steel pallet rack connections", *Eng. Fail. Anal.*, **85**, 149-166. DOI: 10.1016/j.engfailanal.2017.08.014.

Shariati, M., Trung, N.T., Wakil, K., Mehrabi, P., Safa, M. and Khorami, M. (2019d), "Estimation of moment and rotation of steel rack connections using extreme learning machine", *Steel Compos. Struct.*, **31**(5), 427-435. https://doi.org/10.12989/scs.2019.31.5.427.

Shariati, M., Trung, N.T., Wakil, K., Mehrabi, P., Safa, M. and Khorami, M. (2019b), "Moment-rotation estimation of steel rack connection using extreme learning machine.", *Steel Compos. Struct*., **31**(5), 427-435. DOI: https://doi.org/10.12989/scs.2019.31.5.427.

Shi, X., Hassanzadeh-Aghdam, M. and Ansari, R. (2019), "Viscoelastic analysis of silica nanoparticle-polymer nanocomposites", *Compos. Part B: Eng*., **158**, 169-178.

Sinaei, H., Jumaat, M.Z. and Shariati, M. (2011), "Numerical investigation on exterior reinforced concrete Beam-Column joint strengthened by composite fiber reinforced polymer (CFRP)", *Int. J. Phys. Sci*., **6**(28), 6572-6579. DOI: 10.5897/IJPS11.1225.

Systèmes, D. (2007), "Abaqus analysis user's manual", Simulia Corp. Providence, RI, USA.

Taheri, E., Firouzianhaji, A., Usefi, N., Mehrabi, P., Ronagh, H. and Samali, B. (2019), "Investigation of a method for strengthening perforated cold-formed steel profiles under compression loads", *Appl. Sci*., **9**(23), 5085.https://doi.org/10.3390/app9235085.

Tahmasbi, F., Maleki, S., Shariati, M., Ramli Sulong, N.H. and Tahir, M.M. (2016), "Shear capacity of C-shaped and L-shaped angle shear connectors", PLoS One, **11**(8), e0156989. DOI: 10.1371/journal.pone.0156989.

Tao, Z., Han, L.H. and Wang, Z.B. (2005), "Experimental behaviour of stiffened concrete-filled thin-walled hollow steel structural (HSS) stub columns", *J. Constr. Steel Res*., **61**(7), 962-983. https://doi.org/10.1016/j.jcsr.2004.12.003.

Tasdemir, M., Tasdemir, C., Akyüz, S., Jefferson, A., Lydon, F. and Barr, B. (1998), "Evaluation of strains at peak stresses in concrete: a three-phase composite model approach", *Cement Concrete Compos*., **20**(4), 301-318. https://doi.org/10.1016/S0958-9465(98)00012-2.

Trung, N.T., Alemi, N., Haido, J.H., Shariati, M., Baradaran, S. and Yousif, S.T. (2019a), "Reduction of cement consumption by producing smart green concretes with natural zeolites", *Smart Struct. Syst.*, **24**(3), 415-425. https://doi.org/10.12989/sss.2019.24.3.415.

Trung, N.T., Shahgoli, A.F., Zandi, Y., Shariati, M., Wakil, K., Safa, M. and Khorami, M. (2019b), "Moment-rotation prediction of precast beam-to-column connections using extreme learning machine", *Struct. Eng. Mech*., **70**(5), 639-647. https://doi.org/10.12989/sem.2019.70.5.639.

Usefi, N., Sharafi, P. and Ronagh, H. (2019), "Numerical models for lateral behaviour analysis of cold-formed steel framed walls: State of the art, evaluation and challenges", *Thin-Wall. Struct.*, **138**, 252-285. DOI: https://doi.org/10.1016/j.tws.2019.02.019.

Wei, X., Shariati, M., Zandi, Y., Pei, S., Jin, Z., Gharachurlu, S., Abdullahi, M., Tahir, M. and Khorami, M. (2018), "Distribution of shear force in perforated shear connectors", *Steel Compos. Struct.*, **27**(3), 389-399. http://dx.doi.org/10.12989/scs.2018.27.3.389.

Xiao, Q., Teng, J. and Yu, T. (2010), "Behavior and modeling of confined high-strength concrete", *J. Compos. Constr*., **14**(3), 249-259. https://doi.org/10.1061/(ASCE)CC.1943-5614.0000070.

Xie, Q., Sinaei, H., Shariati, M., Khorami, M., Mohamad, E.T. and Bui, D.T. (2019), "An experimental study on the effect of CFRP on behavior of reinforce concrete beam column connections", *Steel Compos. Struct*., **30**(5), 433-441. http://dx.doi.org/10.12989/scs.2019.30.5.433.

Xu, C., Zhang, X., Haido, J.H., Mehrabi, P., Shariati, A., Mohamad, E.T., Hoang, N. and Wakil, K. (2019), "Using genetic algorithms

method for the paramount design of reinforced concrete structures", *Struct. Eng. Mech.*, **71**(5), 503-513. https://doi.org/10.12989/sem.2019.71.5.503.

Xu, C., et al. (2019), "Using genetic algorithms method for the paramount design of reinforced concrete structures", *Struct. Eng. Mech.*, **71**(5), 503-513. https://doi.org/10.12989/sem.2019.71.5.503.

Zandi, Y., Shariati, M., Marto, A., Wei, X., Karaca, Z., Dao, D., Toghroli, A., Hashemi, M.H., Sedghi, Y. and Wakil, K. (2018), "Computational investigation of the comparative analysis of cylindrical barns subjected to earthquake", *Steel Compos. Struct.*, **28**(4), 439-447. http://dx.doi.org/10.12989/scs.2018.28.4.439.

Zeghiche, J. (2013), "Further tests on thin steel and composite fabricated stubs", *J. Constr. Steel Res.*, **81**, 124-137. https://doi.org/10.1016/j.jcsr.2012.11.006.

Zhang, J.H. and Young, B. (2018), "Finite element analysis and design of cold-formed steel built-up closed section columns with web stiffeners", *Thin-Wall. Struct.*, **131**, 223-237. https://doi.org/10.1016/j.tws.2018.06.008.

Ziaei-Nia, A., Shariati, M. and Elnaz, S. (2018), "Dynamic mix design optimization of high-performance concrete", *Steel Compos. Struct.*, **29**(1), 67-75. 10.12989/scs.2018.29.1.067.

CC